

Nonequilibrium phase transitions and finite-size scaling in weighted scale-free networks

Márton Karsai,¹ Róbert Juhász,² and Ferenc Iglói^{3,1}¹*Institute of Theoretical Physics, Szeged University, H-6720 Szeged, Hungary*²*Theoretische Physik, Universität des Saarlandes, D-66041 Saarbrücken, Germany*³*Research Institute for Solid State Physics and Optics, H-1525 Budapest, P.O.Box 49, Hungary*

(Received 26 April 2005; revised manuscript received 5 October 2005; published 13 March 2006)

We consider nonequilibrium phase transitions, such as epidemic spreading, in weighted scale-free networks, in which highly connected nodes have a relatively smaller ability to transfer infection. We solve the dynamical mean-field equations and discuss finite-size scaling theory. The theoretical predictions are confronted with the results of large scale Monte Carlo simulations on the weighted Barabási-Albert network. Local scaling exponents are found different at a typical site and at a node with very large connectivity.

DOI: [10.1103/PhysRevE.73.036116](https://doi.org/10.1103/PhysRevE.73.036116)

PACS number(s): 89.75.Hc, 64.60.Ht, 05.70.Ln

I. INTRODUCTION

Complex networks, which have a more complicated topology than periodic lattices have been observed in a large class of systems in different fields of science, technics, transport, social and political life, etc., see Refs. [1–3] for recent reviews. The structure of complex networks is described by graphs [4], in which the nodes represent the agents and the edges the possible interactions. Generally there are connections between remote sites, too, which is known as the small world effect [5]. Another feature of many real networks is the nondemocratic way of the distribution of the links: there are sites which are much more connected than the average and the distribution of the number of edges, $P(k)$, has a power-law tail

$$P_D(k) \approx Ak^{-\gamma}, \quad k \gg 1, \quad (1)$$

thus the edge distribution is scale free. In real networks the degree exponent is generally: $2 < \gamma < 3$ and as shown by Barabási and Albert [6] scale-free networks are usually the results of growth and preferential attachment.

Since the agents of a network interact in one or another way it is natural to ask about the cooperative behavior of the system. In particular if there exist some kind of (thermodynamical) phases and if there are singular points as the strength of the interaction or other suitable parameter (such as the strength of disordering field, temperature, etc.) are varied. In this respect static models [7–10] (Ising, Potts models, etc.), as well as nonequilibrium processes [11–13] (percolation, spread of epidemics, etc.) are investigated. Generally nonweighted networks are considered, in which the strength of interaction at each bond is constant. Due to long-range interactions conventional mean-field behavior is expected to hold, at least if the network is sufficiently weakly connected, so that the degree exponent is larger than a threshold value, $\gamma > \gamma_u$. For the Ising model this limiting value is given by $\gamma_u = 5$, whereas for the percolation and epidemic spreading it is $\gamma_u = 4$ and at $\gamma = \gamma_u$ there are logarithmic corrections to the mean-field singularities. For lower values of γ , such that $\gamma_u > \gamma > \gamma_c$, where γ_c is a lower threshold value, we arrive to the unconventional mean-field regime in which the critical exponents are γ dependent. The effect of

topology of scale-free networks becomes dramatic if γ is lowered below the lower threshold value, $\gamma \leq \gamma_c$, when the average of k^2 , defined by $\langle k^2 \rangle = \int P_D(k) k^2 dk$, as well as the strength of the average interaction becomes divergent. Consequently in this regime for any finite value of the interaction scale-free networks are in the ordered state, c.f., there is no threshold value of epidemic spreading. Since $\gamma_c = 3$, in realistic networks with homogeneous interactions always this type of phenomena should occur.

Recently, much attention has been paid to weighted networks, in which the interactions are not homogeneous. Generally the strength of interactions of highly connected sites are comparatively weaker than the average, which can be explained by technical or geographical limitations. To model epidemic spreading one should keep in mind that sites with a large coordination number are generally earlier connected to the network and in the long period of existence they have a larger chance to be cured and one can expect that their ability to transfer infection is comparatively smaller [14].

An interesting class of degraded networks has been introduced recently by Giuraniuc *et al.* [15] in which the strength of interaction in a link between sites i and j is rescaled as

$$\lambda_{i,j} = \lambda \frac{(k_i k_j)^{-\mu}}{\langle k^{-\mu} \rangle^2}, \quad (2)$$

where k_i and k_j are the connectivities in the given sites. Here $0 < \mu < 1$ is the degradation exponent and formally with $\mu = 0$ we recover the nondegraded network with homogeneous interaction, λ . The properties of this type of network in equilibrium critical phenomena, in particular for the Ising model have been studied in detail in Ref. [15]. Most interestingly the equilibrium critical behavior is found to depend only on one parameter the effective degree exponent

$$\gamma' = (\gamma - \mu)/(1 - \mu), \quad (3)$$

thus topology and interaction seem to be converted. One important aspect of the degraded network in Eq. (2) that phase transition in realistic networks with $\gamma \leq 3$ is also possible, if the degradation exponent is sufficiently large: $\mu > (3 - \gamma)/2$. Therefore theoretical predictions about critical singularities can be confronted with the results of numerical calculations.

In this paper we study nonequilibrium phase transitions in weighted networks. Our aim with these investigations is twofold. First, we want to check if the simple reparametrization rule in Eq. (3) stays valid for nonequilibrium phase transitions, too. For this purpose we make dynamical mean-field calculations and perform large scale Monte Carlo simulations. Our second aim is to study the form of finite-size scaling in nonequilibrium phase transitions in weighted scale-free networks. To analyze our numerical results we use recent field-theoretical calculations [16] in which finite-size scaling in Euclidean lattices above the upper critical dimension has been studied. In the conventional mean-field regime of scale-free networks analogous scaling relations are expected to apply.

The structure of the paper is the following. The dynamical mean-field solution of the problem is presented in Sec. II, whereas finite-size scaling theory is shown in Sec. III. Results of Monte Carlo simulations of the contact process on weighted Barabási-Albert networks are presented in Sec. IV and discussed in Sec. V.

II. DYNAMICAL MEAN-FIELD SOLUTION

In the calculation we consider the contact process [17], which is the prototype of a nonequilibrium phase transition in the directed percolation universality class [18]. In this process site i of the network is either vacant (\emptyset) or occupied by at most one particle (A). The dynamics of the model is given by a continuous time Markov process and is therefore defined in terms of transition rates. The reactions in the system are of two types: (a) branching in which particles are created at empty sites (provided one of its neighbors, j , is occupied) occurs with rate $\lambda_{i,j}$, (b) death of particles with a rate, κ . This latter rate we set $\kappa=1$. In this section we solve the problem in the mean-field approximation, which is expected to be exact, due to long-range interactions in the system.

We start with the set of equations for the time derivative of the mean-value of the density, ρ_i , at site, $i=1, 2, \dots, N$

$$\frac{\partial \rho_i}{\partial t} = \sum_j \lambda_{i,j} (1 - \rho_i) \rho_j - \rho_i, \quad (4)$$

and correlations in the densities at different sites are omitted. In the next step in the spirit of the mean-field approach we replace the interactions

$$\lambda_{i,j} = \lambda \frac{k_i k_j (k_i k_j)^{-\mu}}{\sum_j k_j \langle k^{-\mu} \rangle^2}, \quad (5)$$

i.e., there is an interaction between each site the (mean) value of which is proportional to the probability of the existence of that bond. Now in terms of an average density

$$\rho = \frac{\sum_j k_j^{1-\mu} \rho_j}{\sum_j k_j^{1-\mu}}, \quad (6)$$

the dynamical mean-field equations in Eq. (4) are given by

$$\frac{\partial \rho_i}{\partial t} = \tilde{\lambda} k_i^{1-\mu} (1 - \rho_i) \rho - \rho_i, \quad (7)$$

with $\tilde{\lambda} = \lambda \langle k^{1-\mu} \rangle / \langle k \rangle \langle k^{-\mu} \rangle^2$. In the stationary state, $\partial \rho_i / \partial t = 0$, the local densities are given by

$$\rho_i = \frac{\tilde{\lambda} k_i^{1-\mu} \rho}{1 + \tilde{\lambda} k_i^{1-\mu} \rho}, \quad (8)$$

i.e., they are proportional to $k_i^{1-\mu}$. Putting ρ_i from Eq. (8) into Eq. (6) we obtain an equation for ρ

$$\langle k^{1-\mu} \rangle = \tilde{\lambda} \int_{k_{\min}}^{k_{\max}} P_D(k) \frac{k^{2(1-\mu)}}{1 + \tilde{\lambda} k^{1-\mu} \rho} dk, \quad (9)$$

where summation over i is replaced by an integration over the degree distribution, $P_D(k)$, and in the thermodynamic limit the upper limit of the integration is $k_{\max} \rightarrow \infty$. The solution of Eq. (9) in the vicinity of the transition point, $\rho \ll 1$, depends on the large- k limit of the degree distribution in Eq. (1) and is given in terms of the integration variable, $k' = k^{1-\mu}$, as

$$\langle k' \rangle = \tilde{\lambda} A \int_{k'_{\min}}^{k'_{\max}} k'^{-\gamma'} \frac{k'^2}{1 + \tilde{\lambda} k' \rho} dk' \equiv Q(\rho, \gamma'), \quad \rho \ll 1, \quad (10)$$

where γ' is defined in Eq. (3). Note, that the functional form of the equation in (10) is identical to that for standard scale-free networks, just with an effective degree exponent, γ' . Thus the solution in Ref. [12] can be applied and in this way we have obtained an extension of the results in Ref. [15] for nonequilibrium phase transitions.

To analyze the solution of Eq. (10) we apply the method in Ref. [9], which is somewhat different from the original method in Ref. [12].

(1) $\gamma' > 4$. For small ρ , $Q(\rho, \gamma')$ in Eq. (10) can be expanded in a Taylor series at least up to a term with $\sim \rho^2$. Consequently there is a finite transition point, $\tilde{\lambda}_c = \langle k' \rangle / A \langle k'^2 \rangle$, and the density in the vicinity of the transition point behaves as: $\rho(\lambda) \sim (\lambda - \lambda_c)$. This is the conventional mean-field regime. At the borderline case, $\gamma' = 4$, there are logarithmic corrections to the mean-field singularities.

(2) $3 < \gamma' < 4$. For small ρ only the linear term in the Taylor expansion of $Q(\rho, \gamma')$ exists. The ρ dependence of the next term, $a_2(\rho)$, is singular and given by

$$a_2(\rho) = -\tilde{\lambda}^2 \rho A \int_{k'_{\min}}^{k'_{\max}} k'^{-\gamma'} \frac{k'^3}{1 + \tilde{\lambda} k' \rho} dk'. \quad (11)$$

The ρ dependence can be estimated by noting that for a small, but finite ρ there is a cutoff value, $\tilde{k}' \sim 1/\rho$, so that

$$a_2(\rho) \sim -\tilde{\lambda}^2 \rho A \int_{k'_{\min}}^{\tilde{k}'} k'^{-\gamma'} k'^3 dk' \sim \rho^{\gamma'-3}. \quad (12)$$

Consequently the density at the transition point behaves anomalously

$$\rho \sim (\lambda - \lambda_c)^\beta, \quad \beta = 1/(\gamma' - 3). \quad (13)$$

This is the unconventional mean-field region.

(3) $\gamma' < 3$. In this case $Q(\rho, \gamma)$ is divergent for small ρ . Its behavior can be estimated as in Eq. (12) leading to $Q(\rho, \gamma') \sim \lambda^{\gamma'-2} \rho^{\gamma'-3}$. Consequently the system for any non-zero value of λ is in the active phase. As λ goes to zero the density vanishes as

$$\rho \sim \lambda^{(\gamma'-2)/(3-\gamma')}. \quad (14)$$

Here at the border, $\gamma' = 3$, the system is still in the active phase, but the density is related to a small λ as: $|\ln(\rho\lambda)| \sim 1/\lambda$.

Before we confront these analytical predictions with the results of numerical simulations we discuss the form of finite-size scaling in scale-free networks.

III. FINITE-SIZE SCALING

In a numerical calculation, such as in Monte Carlo (MC) simulations, one generally considers systems of finite extent and the properties of the critical singularities are often deduced via finite-size scaling. It is known in the phenomenological theory of equilibrium critical phenomena that due to the finite size of the system, L , critical singularities are rounded and their position is shifted [19]. As it is elaborated for Euclidean lattices finite-size scaling theory has different forms below and above the upper critical dimension, d_c . For $d < d_c$ in the scaling regime the singularities are expected to depend on the ratio, L/ξ , where ξ is the spatial correlation length in the infinite system [20]. On the other hand for $d > d_c$, when mean-field theory provides exact values of the critical exponents, finite-size scaling theory involves dangerous irrelevant scaling variables [21], which results in the breakdown of hyperscaling relations. For equilibrium critical phenomena predictions of finite-size scaling theory [22] above d_c are checked numerically, but the agreement is still not satisfactory [23].

For nonequilibrium critical phenomena finite-size scaling above d_c is considered first in the frame of scaling theory [24] and for the percolation process [25] and applied also for a coupled directed percolation system [26]. A field-theoretical derivation of the results has been made only very recently [16] and here we recapitulate the main findings of the analysis. For directed percolation, which represents a broad class of universality [27], dangerous irrelevant scaling variables are identified in the fixed point. As a consequence scaling of the order parameter is anomalous

$$\rho = L^{-\beta/\nu^*} \tilde{\rho}(\delta L^{1/\nu^*}, h L^{\Delta/\nu^*}). \quad (15)$$

Here, δ , is the reduced control parameter, with the notations of Sec. II $\delta = (\lambda - \lambda_c)/\lambda_c$ and h is the strength of an ordering field. The critical exponents, $\beta = 1$ and $\Delta = 2$, are the same as in conventional mean-field theory. The finite-size scaling exponent is given by, $\nu^* = 2/d$, and thus depends on the spatial dimension, d . Note, that below $d_c = 4$ it is the correlation length exponent, ν , which enters into the scaling expression in Eq. (15), but above d_c , due to dangerous irrelevant scaling

variables it should be replaced by ν^* . At the critical point, $\delta = 0$, the scaling function, $\tilde{\rho}(0, x)$, has been analytically calculated and checked by numerical calculations.

In the following we translate the previous results for complex network, in which finite-size scaling is naturally related to the volume of the network, which is given by the number of sites, N . In the conventional mean-field regime with the correspondence, $N \leftrightarrow L^d$, we arrive from Eq. (15) to the finite-size scaling prediction

$$\rho_{typ} = N^{-\beta/2} \tilde{\rho}_{typ}(\delta N^{1/2}, h N^{\Delta/2}), \quad (16)$$

which is expected to hold for a typical site, i.e., with a coordination number, $k \sim \langle k \rangle$. On the other hand for the maximally connected site with $k_{max} \sim N^{1/(\gamma-1)}$ according to Eq. (8) the finite-size scaling form is modified by

$$\rho_{max} = N^{-\beta/2 + (1-\mu)/(\gamma-1)} \tilde{\rho}_{max}(\delta N^{1/2}, h N^{\Delta/2}). \quad (17)$$

Since in the derivation of the relation in Eq. (15) the actual value of β has not been used, we conjecture that the results in Eqs. (16) and (17) remain valid in the unconventional mean-field region, too.

IV. MONTE CARLO SIMULATION

In the actual calculation we considered the contact process on the Barabási-Albert scale-free network [6], which has a degree exponent, $\gamma = 3$, and used a degradation exponent, $\mu = 1/2$. Consequently from Eq. (3) the effective degree exponent is $\gamma' = 5$, thus conventional mean-field behavior is expected to hold. (We note that the same system is used to study the equilibrium phase transition of the Ising model in Ref. [15].) Networks of sites up to $N = 4096$ are generated by starting with $m_0 = 1$ node and having an average degree: $\langle k \rangle = 2$. Results are averaged over typically 10 000 independent realizations of the networks.

In the calculation we started with a single particle at site i (which was either a typical site or the maximally connected site) and let the process evolve until a stationary state is reached in which averages become time independent. In a finite system in particular in the vicinity of the critical point this state is only quasistationary and has a finite life time before in the system all particles are annihilated. In order to obtain a true (quasi)stationary average value we have considered only those samples which have survived up to the time where the average is done [28]. In the calculation we monitored the average value of the occupation number, ρ_i , as introduced in the mean-field theory in Eq. (4), and the fraction of occupied sites, m_i (order parameter) as a function of λ , whereas κ was set to be unity. In a regular lattice in the stationary state and in the thermodynamic limit ρ_i and m_i are the same quantities. In a complex network, however, in which the ρ_i are position dependent they are not strictly equivalent. Their singular behavior in the vicinity of the transition point, however, is expected to be the same [29].

The λ dependence of the order parameter is shown in Fig. 1 for a typical site and in Fig. 2 for the maximally connected site. Evidently there is a phase transition in the system in the thermodynamic limit, which is rounded by finite size effects as shown in the insets of Figs. 1 and 2.

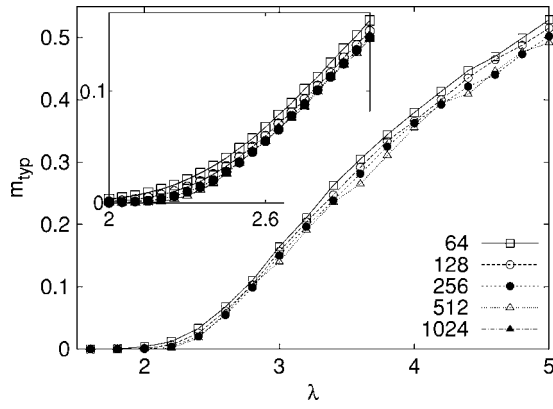


FIG. 1. Variation of the order parameter at a typical site as a function of the creation rate, λ . Inset: Enlargement in the critical region.

To locate the phase transition point we form the ratios: $r(N)=m(N)/m(N/2)$, for different finite sizes. As shown in Fig. 3 $r(N)$ tends to zero in the inactive phase, $\lambda < \lambda_c$, and tends to a value of one in the active phase, $\lambda > \lambda_c$. The curves for different N cross each other and the crossing point can be used to identify λ_c through extrapolation. Furthermore the value of the ratio at the critical point is given by: $r(N, \lambda_c) = 2^{-x}$, where x is the finite-size scaling exponent, as given in scaling theory in Eqs. (16) and (17).

The transition point is found to be the same within the error of the calculation both for a typical site and for the maximally connected site and given by: $\lambda_c = 2.30(1)$. The finite-size scaling exponent, however, calculated from $r(N, \lambda_c)$ is different in the two cases. For a typical site we estimate: $x_{typ} = 0.54(7)$, which should be compared with the field-theoretical prediction in Eq. (16), which is $x_{typ} = \beta/2 = 1/2$. In the maximally connected site the finite-size scaling exponent is measured as $x_{max} = 0.27(4)$, which again agrees well with the field-theoretical prediction in Eq. (17): $x_{max} = \beta/2 - (1 - \mu)/(\gamma - 1) = \beta/2 - 1/(\gamma' - 1) = 1/4$.

Next, we consider correlations in the vicinity of the transition point and calculate the relation between the correlated volume, \mathcal{V} , and the distance from the critical point, δ , which is expected to be in a power-law form, $\mathcal{V} \sim |\delta|^{-\omega}$. According to field-theoretical results in Eqs. (16) and (17) this exponent is $\omega = 2$, both at a typical site and at the maximally connected

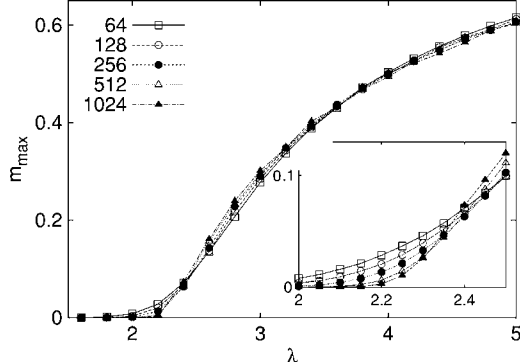


FIG. 2. As in Fig. 1 for the maximally connected site.

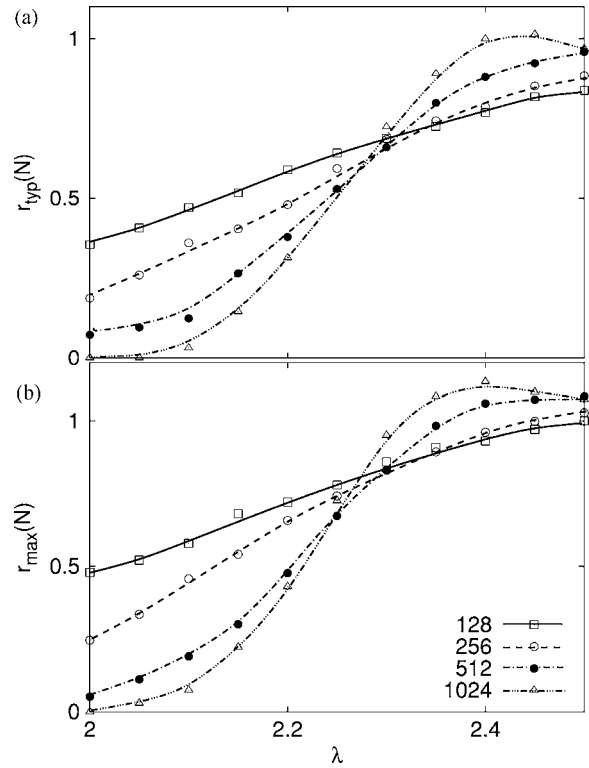


FIG. 3. The ratio $r(N)=m(N)/m(N/2)$ (a) for a typical site, (b) for the maximally connected site. Note that the location of the crossing points, which defines λ_c is the same in the two cases, whereas the value at crossing, which is related to the finite-size exponent, x , through $r(N, \lambda_c) = 2^{-x}$ is different.

site. Now in the limiting case, $\mathcal{V} \sim N$, the scaled order parameter, $\tilde{m} = mN^x$, is expected to depend on the scaling combination, $N^{1/\omega} \delta$, which is demonstrated in Fig. 4, both in the typical site (a) and in the maximally connected site (b). In both cases x and λ_c are fixed by the previous analysis and ω is obtained from the optimal scaling collapse, as $\omega_{typ} = 2.1(2)$ and $\omega_{max} = 2.0(1)$. Thus, once more we have agreement with the field-theoretical results.

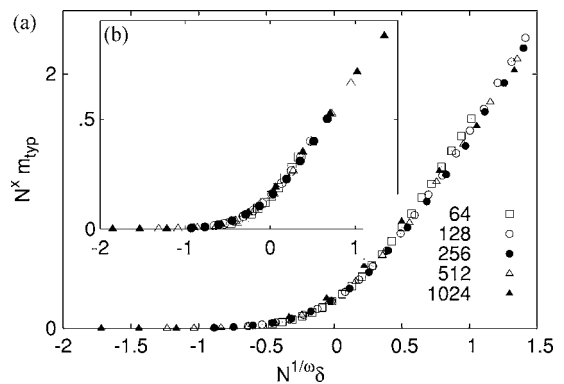


FIG. 4. Scaling collapse of the order parameter near the transition point using the functional forms in Eq. (16) for a typical site (a) and in Eq. (17) for the maximally connected site (b). The finite-size scaling exponents, x_{typ} and x_{max} are fixed by the previous analysis and the correlation exponent, ω , is used to have an optimal collapse of the data, see text.

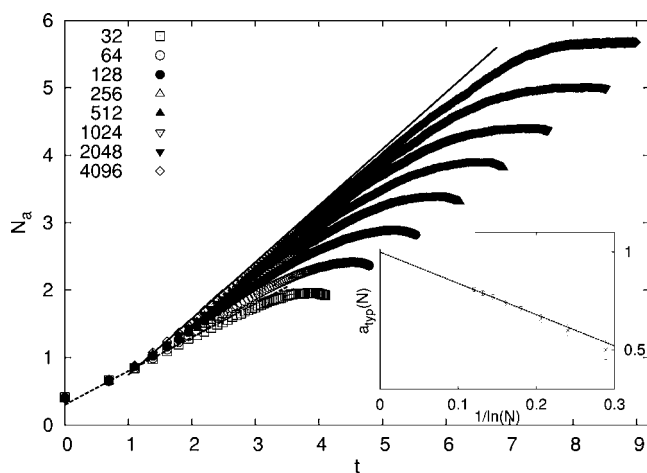


FIG. 5. Time dependence of the number of active sites starting from a typical site at the critical point in a log-log scale. For $t > N^\zeta$, when the infection has reached the border of the system the curves are saturated. The slope of the limiting curve for $N \rightarrow \infty$ defines a_{typ} . The full straight line with slope 0.84 fits the largest finite-size data. For small sizes there is a cross over and the local slope of the curves is $a_{max} \approx 0.5$, see text. Here the broken straight line has a slope of $1/2$. Extrapolation of the finite-size slopes, $a_{typ}(N)$, as a function of $1/\ln N$ is shown in the inset.

Finally, we turn to analyze dynamical scaling in the system. At the critical point, $\lambda = \lambda_c$ we have measured the number of active sites, N_a , as a function of time, t , which is shown in Fig. 5 when the starting point is a typical site and in Fig. 6 for the maximally connected site. As seen in Figs. 5 and 6 after a starting period (which is discussed below) there is an asymptotic region with a power-law dependence, $N_a \sim t^a$, which turns to a saturation regime around $t \sim N^\zeta$, when the active sites reach the boundary of the system. It is seen in Figs. 5 and 6 that the exponents a_{typ} and a_{max} , which refer to a typical site and the maximally connected site, respectively, are different. However the border of the saturation regions, i.e., the exponent ζ are approximately the same

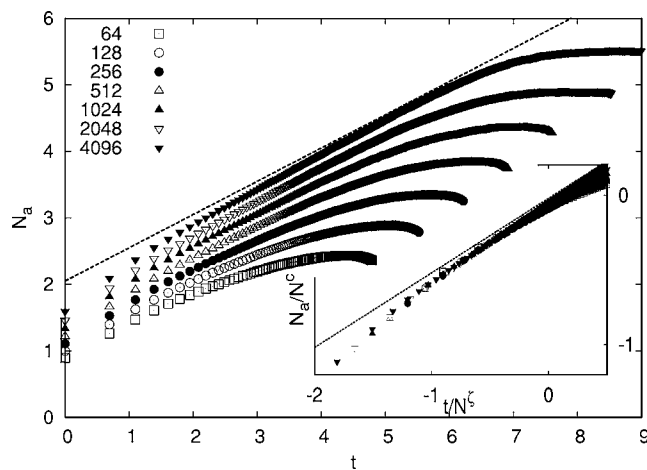


FIG. 6. The same as in Fig. 5 for the maximally connected site. Inset: scaling collapse of N_a/N^c versus t/N^ζ in a log-log plot with $c=0.5$ and $\zeta_{max}=0.5$. The slope of the straight lines both in the main panel and in the inset indicates the prediction $a_{max}=1/2$.

for the two cases. In a regular lattice with dimension, $d > d_c$, (which contains only typical sites) the dynamical exponent, ζ , is conjectured [24] to be, $\zeta=1/2$, which is derived recently by field-theoretical methods [16] and checked numerically [30]. This result for ζ is expected to hold for networks, too.

In order to analyze the results in Figs. 5 and 6 we discuss the scaling behavior of $N_a(t, N)$. In the stationary state the density is independent of the initial conditions and it is proportional to the density at a typical site, $\rho_{typ} \sim N^{-x_{typ}}$. Therefore the scaling form of the number of active sites is given by

$$N_a(t, N) = N^{1-x_{typ}} \tilde{N}_a(t/N^\zeta), \quad (18)$$

in which the scaling function, $\tilde{N}_a(y)$, is different for a typical site and for the maximally connected site, respectively. In the small y limit we obtain $\tilde{N}_a(y) \sim y^{a_{typ}}$ and $\tilde{N}_a(y) \sim y^{a_{max}}$, for a typical site and for the maximally connected site, respectively, in this way we recover the previously announced t dependences. For small t , N_a is of $O(1)$, if we start with a particle at a typical site and it is of order of the number of links at the hub, $k_{max}^{1-\mu} \sim N^{1/(\gamma'-1)} \sim N^{x_{typ}-x_{max}}$, if we start at the maximally connected site. Next we analyze the size dependence of $N_a(t, N)$ at a fixed t . For a typical site $\lim_{N \rightarrow \infty} N_a(t, N)$ is expected to have a finite limiting value, which is in accordance with the numerical results in Fig. 5. Indeed for typical sites the size of the network should not influence the local growth in the system. Using the small y behavior of the scaling function we obtain the relation

$$1 - x_{typ} - \zeta_{typ} a_{typ} = 0. \quad (19)$$

For not too large finite systems, however, there is a starting regime and thus a cross-over phenomenon what can be seen in Fig. 5. This cross over is due to the fact that in a small system the infection can reach the maximally connected site in a short time and afterwards the growth is characterized with an exponent $a_{max} < a_{typ}$. This starting region is also indicated in Fig. 5.

For the maximally connected site the number of neighbors and thus the local density depend on the size of the network. As a consequence $N_a(t, N)$ at a fixed t has a size dependence, which can be seen in Fig. 6. Using the result in Eq. (8) we obtain $\lim_{N \rightarrow \infty} N_a(t, N) \sim k_{max}^{1-\mu} \sim N^{1/(\gamma'-1)} \sim N^{x_{typ}-x_{max}}$. Now comparing the N dependence for small t leads to the relation

$$1 - x_{typ} - \zeta_{max} a_{max} = x_{typ} - x_{max}. \quad (20)$$

The exponent, a_{typ} , can be obtained from the asymptotic slope of the master curve in Fig. 5, which has a strong size dependence. Extrapolation as shown in the inset of Fig. 5 gives $a_{typ}=0.95(10)$ which is compatible with the mean-field and finite-size scaling prediction, $a_{typ}=1$. For the maximally connected site in Fig. 6 the slope of the curves have a weaker size dependence and can be estimated as: $a_{max}=0.52(4)$. Consequently from the relations in Eqs. (19) and (20) we obtain that both ζ_{typ} and ζ_{max} are compatible with the mean-field prediction, $\zeta=1/2$. From these results, using $N \sim \delta^{-\omega}$, we obtain for the scaling behavior of the relaxation time, τ ,

in the vicinity of the transition point, $\tau \sim \delta^{-\nu_{\perp}}$, with $\nu_{\perp} = \zeta\omega$, so that $\nu_{\perp} = 0.95(10)$ both for the typical and the maximally connected sites, in complete agreement with the mean-field and finite-size scaling result, $\nu_{\perp} = 1$.

The scaling prediction for $N_a(t, N)$ for small t is checked for the maximally connected site in the inset of Fig. 6. Here N_a/N^c is plotted as a function of t/N^{ζ} . There is an appropriate scaling collapse with the mean-field values: $c = 1 - x_{typ} = 0.5$ and $\zeta_{max} = 0.5$.

V. DISCUSSION

We considered nonequilibrium phase transitions in weighted scale-free networks, in which the creation rate of particles at given sites is rescaled with a power of the connectivity number. In this way nonequilibrium phase transitions are realized even in realistic networks having a degree exponent, $\gamma \leq 3$. Mean-field theory, which is generally believed to be exact in these lattices, is solved and the previously known three regimes of criticality (conventional and unconventional mean-field behavior, as well as only active phase) are identified. The theoretical predictions in the conventional mean-field regime are confronted with the results of Monte Carlo simulations of the contact process on the

weighted Barabási-Albert network. To analyze the simulation results we have applied and generalized recent field-theoretical results [16] about finite-size scaling of nonequilibrium phase transitions above the upper critical dimension, i.e., in the mean-field regime. For a network the natural variable is the volume (mass) of the system which enters in a simple way into the scaling combinations. We have obtained overall agreement with this finite-size scaling theory in which the critical exponents are simple rational numbers. We have also numerically demonstrated that at sites with very large connectivity there are new local scaling exponents, which differ from the values measured at a typical site.

ACKNOWLEDGMENTS

F.I. is indebted to S. Lübeck for useful discussions and for sending a copy of Refs. [16,30] before publication. This work has been supported by a German-Hungarian exchange program (DAAD-MÖB), by the Hungarian National Research Fund under Grant Nos. OTKA TO34138, TO37323, TO48721, MO45596, and M36803. M.K. thanks to the Institute of Theoretical Physics, University of Saarland and to Professor H. Rieger for hospitality during an Erasmus exchange. R.J. acknowledges support by the Deutsche Forschungsgemeinschaft under Grant No. SA864/2-1.

-
- [1] R. Albert and A. L. Barabási, *Rev. Mod. Phys.* **74**, 47 (2002).
 [2] S. N. Dorogovtsev and J. F. F. Mendes, *Adv. Phys.* **51**, 1079 (2002).
 [3] S. N. Dorogovtsev and J. F. F. Mendes, *Evolution of Networks: From Biological Nets to the Internet and WWW* (Oxford University Press, Oxford, 2003).
 [4] B. Bollobás, *Random Graphs* (Academic Press, London, 1985).
 [5] D. J. Watts and S. H. Strogatz, *Nature (London)* **393**, 440 (1998).
 [6] A. L. Barabási and R. Albert, *Science* **286**, 509 (1999).
 [7] A. Aleksiejuk, J. A. Holyst, and D. Stauffer, *Physica A* **310**, 260 (2002).
 [8] M. Leone, A. Vazquez, A. Vespignani, and R. Zecchina, *Eur. Phys. J. B* **28**, 191 (2002); S. N. Dorogovtsev, A. V. Goltsev, and J. F. F. Mendes, *Phys. Rev. E* **66**, 016104 (2002); G. Bianconi, *Phys. Lett. A* **303**, 166 (2002).
 [9] F. Iglói and L. Turban, *Phys. Rev. E* **66**, 036140 (2002).
 [10] S. N. Dorogovtsev, A. V. Goltsev, and J. F. F. Mendes, *Eur. Phys. J. B* **38**, 177 (2004).
 [11] D. S. Callaway, M. E. J. Newman, S. H. Strogatz, and D. J. Watts, *Phys. Rev. Lett.* **85**, 5468 (2000); R. Cohen, D. ben-Avraham, and S. Havlin, *Phys. Rev. E* **66**, 036113 (2002).
 [12] R. Pastor-Satorras and A. Vespignani, *Phys. Rev. Lett.* **86**, 3200 (2001); *Phys. Rev. E* **63**, 066117 (2001).
 [13] M. E. J. Newman, *Phys. Rev. E* **66**, 016128 (2002).
 [14] Z. Dezső and A.-L. Barabási, *Phys. Rev. E* **65**, 055103 (2002).
 [15] C. V. Giuraniuc, J. P. L. Hatchett, J. O. Indekeu, M. Leone, I. Perez Castillo, B. Van Schaebroeck, and C. Vanderzande, *Phys. Rev. Lett.* **95**, 098701 (2005).
 [16] S. Lübeck and H. K. Janssen, *Phys. Rev. E* **72**, 016119 (2005).
 [17] T. E. Harris, *Ann. Probab.* **2**, 969 (1974).
 [18] P. Grassberger and A. de la Torre, *Ann. Phys. (N.Y.)* **122**, 373 (1979).
 [19] M. N. Barber, in *Phase Transitions and Critical Phenomena*, Vol. 8, edited by C. Domb and J. L. Lebowitz (Academic Press, New York, 1984).
 [20] M. E. Fisher and M. N. Barber, *Phys. Rev. Lett.* **28**, 1516 (1972).
 [21] M. E. Fisher, in *Renormalization Group in Critical Phenomena and Quantum Field Theory*, edited by D. J. Gunton and M. S. Green (Temple University, Philadelphia, 1974).
 [22] E. Brézin, *J. Phys. (France)* **43**, 15 (1982); E. Brezén and J. Zinn-Justin, *Nucl. Phys. B* **257**, 867 (1985).
 [23] E. Luijten and H. W. J. Blöte, *Phys. Rev. Lett.* **76**, 1557 (1996); X. S. Chen and V. Dohm, *Eur. Phys. J. B* **5**, 529 (1998); E. Luijten, K. Binder, and H. W. J. Blöte, *Eur. Phys. J. B* **9**, 289 (1999); D. Stauffer, *Braz. J. Phys.* **30**, 787 (2000).
 [24] R. Botet, R. Jullien, and P. Pfeuty, *Phys. Rev. Lett.* **49**, 478 (1982).
 [25] A. Aharony, Y. Gefen, and A. Kapitulnik, *J. Phys. A* **17**, L197 (1984).
 [26] J. D. Noh and H. Park, *Phys. Rev. Lett.* **94**, 145702 (2005).
 [27] H. Hinrichsen, *Adv. Phys.* **49**, 815 (2000).
 [28] T. Aukrust, D. A. Browne, and I. Webman, *Phys. Rev. A* **41**, 5294 (1990).
 [29] Indeed at the critical point the fraction of active sites is vanishing with N , see in Eqs. (16) and (17), therefore starting from a typical site the probability of the infection of a largely connected site is vanishing.
 [30] S. Lübeck (private communication).